THE JOURNAL OF BIOLOGICAL CHEMISTRY VOL. 291, NO. 38, pp. 19746–19759, September 16, 2016

Characterization of Human and Yeast Mitochondrial Glycine Carriers with Implications for Heme Biosynthesis and Anemia*[S]

Received for publication, May 6, 2016, and in revised form, July 29, 2016 Published, JBC Papers in Press, July 30, 2016, DOI 10.1074/jbc.M116.736876

Paola Lunetti[‡], Fabrizio Damiano[‡], Giuseppe De Benedetto[§], Luisa Siculella[‡], Antonio Pennetta[§], Luigina Muto[¶], Eleonora Paradies[‖], Carlo Marya Thomas Marobbio[**], Vincenza Dolce[¶1], and Loredana Capobianco[‡2]

*From the [‡]Department of Biological and Environmental Sciences and Technologies, University of Salento, 73100 Lecce, Italy, [§]Laboratory of Analytical and Isotopic Mass Spectrometry, Department of Cultural Heritage, University of Salento, 73100 Lecce, Italy, [¶]Department of Pharmacy, Health, and Nutritional Sciences, University of Calabria, 87036 Arcavacata di Rende (Cosenza), Italy, [‖]Consiglio Nazionale delle Ricerche, Institute of Biomembranes and Bioenergetics, 70125 Bari, Italy, and **Department of Biosciences, Biotechnology, and Pharmacological Sciences, University of Bari, 70125 Bari, Italy*

Heme is an essential molecule in many biological processes, such as transport and storage of oxygen and electron transfer as well as a structural component of hemoproteins. Defects of heme biosynthesis in developing erythroblasts have profound medical implications, as represented by sideroblastic anemia. The synthesis of heme requires the uptake of glycine into the mitochondrial matrix where glycine is condensed with succinyl coenzyme A to yield δ-aminolevulinic acid. Herein we describe the biochemical and molecular characterization of yeast Hem25p and human SLC25A38, providing evidence that they are mitochondrial carriers for glycine. In particular, the *hem25Δ* mutant manifests a defect in the biosynthesis of δ-aminolevulinic acid and displays reduced levels of downstream heme and mitochondrial cytochromes. The observed defects are rescued by complementation with yeast *HEM25* or human *SLC25A38* genes. Our results identify new proteins in the heme biosynthetic pathway and demonstrate that Hem25p and its human orthologue SLC25A38 are the main mitochondrial glycine transporters required for heme synthesis, providing definitive evidence of their previously proposed glycine transport function. Furthermore, our work may suggest new therapeutic approaches for the treatment of congenital sideroblastic anemia.

Sideroblastic anemias are disorders characterized by erythroblast mitochondrial iron overload (1). There are two forms of sideroblastic anemia: acquired and congenital. Acquired anemia occurs after exposure to certain drugs or alcohol and with copper deficiency (2, 3). Congenital sideroblastic anemia is a rare and heterogeneous disease caused by mutations of genes involved in heme biosynthesis, iron-sulfur (Fe-S) cluster biogenesis, or Fe-S cluster transport and mitochondrial metabolism (2, 4–6). Different forms of Congenital sideroblastic anemia have been defined at the molecular level, each of which has provided some insight into cellular pathways associated with dysfunctional mitochondrial iron metabolism (7). X-linked sideroblastic anemia is a form of non-syndromic congenital sideroblastic anemia caused by a defect of the δ-aminolevulinate synthase 2 (*ALAS2*)[3] gene, which encodes the first mitochondrial enzyme of heme biosynthesis in erythroid cells (8, 9). The ALAS2 catalyzes the condensation into mitochondria of glycine with succinyl-coenzyme A to yield δ-aminolevulinic acid (ALA) and requires pyridoxal 5′-phosphate (PLP; vitamin B6) as the cofactor (10, 11). Following its synthesis, ALA is exported to the cytosol where it is converted to coproporphyrinogen III. All the remaining steps of heme biosynthesis take place inside mitochondria. Coproporphyrinogen III is imported into the mitochondrial intermembrane space where it is converted to protoporphyrinogen IX by coproporphyrinogen oxidase. Then, protoporphyrinogen IX is oxidized to protoporphyrin IX by protoporphyrinogen oxidase. Lastly, ferrous iron is incorporated into protoporphyrin IX to form heme in the mitochondrial matrix, a reaction catalyzed by ferrochelatase (12). Although all the enzymatic steps leading to the production of heme are well characterized, it is still not completely understood how ALA, coproporphyrinogen III, and heme are transported across the two mitochondrial membranes. Recently, Guernsey *et al.* (13) has characterized a subset of patients with severe non-syndromic congenital sideroblastic anemia resembling X-linked sideroblastic anemia but lacking the *ALAS2* mutations (13). In this subgroup of patients the author identified several mutations in the *SLC25A38* gene (13). Furthermore, an anemic phenotype similar to that of *ALAS2* deficiency has also been observed in the knockdown of two zebrafish orthologues of *SLC25A38* (*slc25a38a* and *slc25a38b*), indicating that this gene is important for red blood cell production and function (13, 14). It has been demonstrated that the genetic deletion of the *Saccharomyces cerevisiae SLC25A38* ortholog *YDL119c* (also named *HEM25*) produces a respiratory pheno-

* This work was supported by grants from the Italian Ministry of Education, Universities, and Research (MIUR) (SIR 2015, molecular and pathogenetic mechanism of congenital sideroblastic anemia associated with the SLC25A38 gene deficiency). The authors declare that they have no conflicts of interest with the contents of this article.

[S] This article contains supplemental Fig. S1.

[1] To whom correspondence may be addressed. Tel.: 39-0984493177; Fax: 39-0984493107.

[2] To whom correspondence should be addressed. Tel.: 39-0832298864; Fax: 39-0832298626.

[3] The abbreviations used are: ALAS2, δ-aminolevulinate synthase 2; ALA, δ-aminolevulinic acid; SM, synthetic minimal medium; YP, rich medium; GlyC, glycine carrier; PLP, pyridoxal 5′-phosphate; Cyt, cytochrome.

type, indicative of mitochondrial involvement (13). Furthermore, this yeast deletion strain shows significantly reduced ALA levels, the first product in the heme biosynthetic pathway. Given that ALAS2 function is not altered in the deletion strain, it was speculated that the decrease in ALA levels was because of decreased precursor availability. On the basis of these findings, it was hypothesized that SLC25A38 and its yeast orthologue Hem25p facilitate ALA production by importing glycine into mitochondria or by exchanging glycine for ALA across the inner mitochondrial membrane (13). Furthermore, Fernández-Murray (14) has recently demonstrated through phenotype assessment in *hem25*Δ cells that Hem25p is required to initiate heme synthesis. Human *SLC25A38* and yeast *HEM25* encode a protein of the inner mitochondrial membrane that belongs to the mitochondrial carrier family, a family of proteins (InterPro entry: IPR018108; PANDIT: PF00153) encoded by nuclear genes (15). SLC25A family members mediate the exchange of metabolites across the inner mitochondrial membrane and have a tripartite structure consisting of three tandem-repeated sequences of ~100 amino acids in length (15). Each repeat contains two hydrophobic stretches that span the membrane as α-helices and a characteristic sequence motif (15).

Herein we report the identification and functional characterization of the mitochondrial glycine carrier protein (named Hem25p) encoded by *HEM25* (16). Hem25p was overexpressed in bacteria, reconstituted into phospholipid vesicles, and identified by its transport properties as a glycine carrier. Hem25p functions in yeast mitochondria with properties similar to those observed in the recombinant protein. The cellular localization of the tagged protein was investigated using confocal laser microscopy, and Hem25p was found targeted to mitochondria. The *hem25*Δ mutant also displayed a severe delay in growth on non-fermentable carbon sources. The *hem25*Δ cells exhibited lower levels of glycine and ALA both in their mitochondria and in cell lysates as well as decreased respiratory efficiency resulting from the reduced expression of some protein components of the yeast cytochrome bc_1 complex. Furthermore, the recombinant SLC25A38 protein (henceforth named GlyC, glycine carrier) overexpressed in bacteria and reconstituted into phospholipid vesicles transported glycine, and its gene was able to rescue the growth defect in *hem25*Δ cells. This is the first time that the protein responsible for the uptake of glycine into mitochondria has been identified at the molecular level.

Results

Bacterial Expression of Hem25p—Hem25p was overexpressed at high levels in *Escherichia coli* BL21(DE3) as inclusion bodies and purified by Ni^{2+}-nitrilotriacetic acid-agarose affinity chromatography (Fig. 1*A*, *lanes 4* and *5*). The apparent molecular mass of the purified protein was about 36 kDa (calculated value with initiator methionine 37.3 kDa). The protein was not detected in bacteria harvested immediately before the induction of expression (Fig. 1*A*, *lane 2*) or in cells harvested after induction but lacking the coding sequence in the expression vector (Fig. 1*A*, *lane 3*). Approximately 90 mg of purified protein was obtained per liter of culture. The identity of the purified protein was confirmed by Western blot analysis (Fig. 1*B*, *lanes 4* and *5*).

Functional Characterization of Recombinant Hem25p—Because it has been hypothesized that Hem25p facilitates ALA production by importing glycine into mitochondria (13, 14), the recombinant and purified Hem25p was reconstituted into liposomes, and its ability to transport glycine was tested. Proteoliposomes reconstituted with Hem25p catalyzed active [^{14}C]glycine/glycine exchange, which was abolished by a mixture of the inhibitors PLP and bathophenanthroline (BAT). Reconstituted Hem25p did not catalyze significant homo-exchanges for aspartate, glutamate, glutamine, asparagine, ornithine, lysine, arginine, proline, and threonine (internal concentration, 10 mM; external concentration, 1 mM). No [^{14}C]glycine/glycine exchange was observed with Hem25p that had been boiled before incorporation into liposomes or after reconstitution of sarcosyl-solubilized material from bacterial cells either lacking the expression vector for Hem25p or harvested immediately before the induction of expression.

The substrate specificity of purified and reconstituted Hem25p was investigated in detail by measuring the uptake of [^{14}C]glycine into proteoliposomes that had been preloaded with various potential substrates (Fig. 1*C*). External glycine was significantly exchanged only in the presence of internal glycine. Furthermore, transport activities were also observed with internal sarcosine, L-alanine, and *N*-methyl-L-alanine. A low exchange was found with β-alanine and α-(methylamino)-isobutyric acid, whereas the activity observed with L-serine, ALA, and L-glutamate was approximately the same as that observed in the absence of internal substrate (Fig. 1*C*). Reconstituted Hem25p, therefore, exhibits a very narrow substrate specificity, which is virtually confined to glycine.

The effects of known mitochondrial inhibitors on the [^{14}C]glycine/glycine reaction catalyzed by reconstituted Hem25p were also examined (Fig. 1*D*). The activity of the recombinant protein was markedly inhibited by tannic acid (17), PLP, and bathophenanthroline (18) (known inhibitors of several mitochondrial carriers) as well as by thiol reagents (*p*-hydroxymercuribenzoate, mercuric chloride, and *N*-ethylmaleimide) (18, 19). In addition, no significant inhibition was observed with butylmalonate (20), 1,2,3-benzenetricarboxylate (21), and bongkrekic acid (22), specific inhibitors of the dicarboxylate carrier, citrate carrier, and ADP/ATP carrier, respectively. Also bromcresol purple (17) had no effect on the activity of the yeast reconstituted protein (Fig. 1*D*).

The time-course of uptake by proteoliposomes of 1 mM [^{14}C]glycine measured either as exchange (with 10 mM glycine inside the proteoliposomes) or as uniport (without internal substrate) is shown in Fig. 1*E*. All curves fitted a first-order rate equation with rate constants (*k*) for the exchange and uniport reactions of ~0.18 min^{-1} and 0.11 min^{-1}, respectively. The initial rates of glycine uptake (the product of *k* and intraliposomal quantity of glycine taken up at equilibrium) were about 95.96 ± 4.55 and 16.36 ± 0.72 nmol/min × mg of protein for the exchange and uniport reactions, respectively. The addition of 10 mM unlabeled glycine to proteoliposomes after incubation with 1 mM [^{14}C]glycine for 30 min, when radioactive uptake had almost reached equilibrium, caused an extensive efflux of

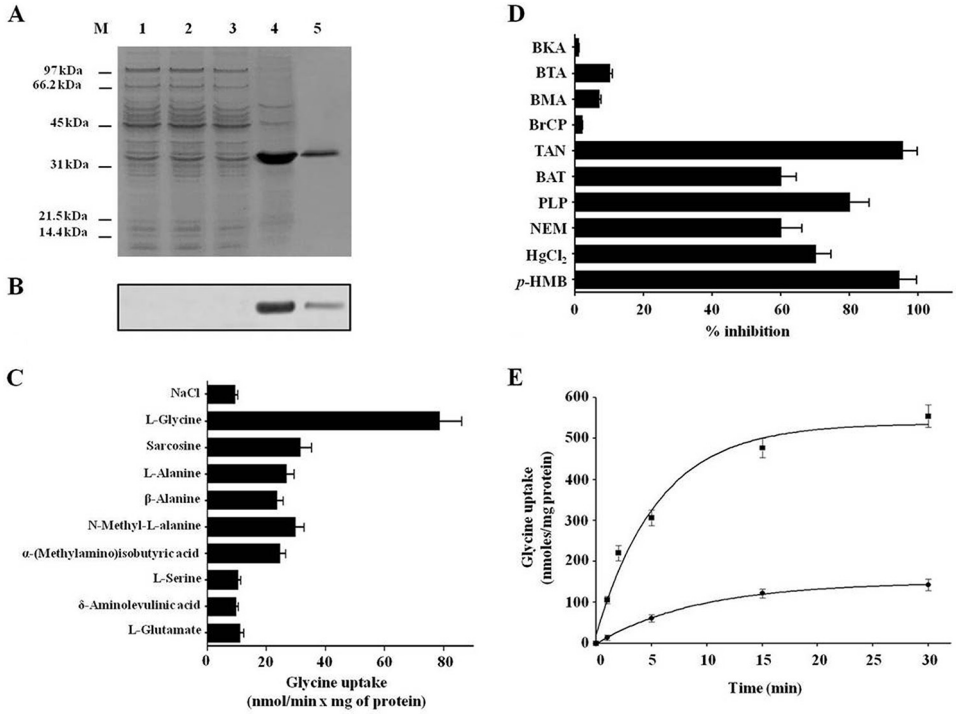

FIGURE 1. **Hem25p catalyzes glycine transport.** *A* and *B*, expression in *E. coli* and purification of Hem25p. Proteins were separated by SDS-PAGE and stained with Coomassie Blue dye (*A*) or transferred to nitrocellulose and immunodetected with an anti-V5 monoclonal antiserum (*B*). *Lane M*, markers (phosphorylase *b*, serum albumin, ovalbumin, carbonic anhydrase, trypsin inhibitor, and lysozyme); *lanes 1–4*, *E. coli* BL21(DE3) containing the expression vector, without (*lanes 1* and *3*) and with (*lanes 2* and *4*) the coding sequence for Hem25p. Samples were taken at the time of induction (*lanes 1* and *2*) and 1 h later (*lanes 3* and *4*). The same number of bacteria was analyzed in each sample. *Lane 5*, purified Hem25p (5 μg) originating from bacteria shown in *lane 4*. *C*, dependence of Hem25p transport activity on internal substrate. Proteoliposomes were preloaded internally with various substrates (concentration 10 mM). Transport was started by adding 0.75 mM [^{14}C]glycine to proteoliposomes reconstituted with Hem25p and terminated after 1 min. Data are the means ± S.D. of at least five independent experiments. *D*, effect of inhibitors on the [^{14}C]glycine/glycine exchange mediated by Hem25p. Proteoliposomes were preloaded internally with 10 mM glycine. Transport was initiated by adding 0.75 mM [^{14}C]glycine to proteoliposomes reconstituted with Hem25p and was stopped after 1 min. The inhibitors were added 3 min before the labeled substrate. The final concentrations of the inhibitors were 10 mM (*BAT*, bathophenanthroline), 2 mM (*BTA*, 1,2,3-benzenetricarboxylate; *BMA*, butylmalonate), 1 mM (*NEM*, *N*-ethylmaleimide), 100 μM (*p-HMB*, *p*-hydroxymercuribenzoate; *BrCP*, bromcresol purple), 10 μM (*BKA*, bongkrekic acid), and 0.1% (w/v) (*TAN*, tannic acid). The extent of inhibition (%) from a representative experiment is reported. Similar results were obtained in at least five experiments. *E*, kinetics of [^{14}C]glycine transport in proteoliposomes reconstituted with Hem25p. 1 mM [^{14}C]glycine was added to proteoliposomes containing 10 mM glycine (exchange, *solid squares*) or 10 mM NaCl and no substrate (uniport, *solid circles*). Similar results were obtained in five independent experiments.

radiolabeled glycine from both glycine-loaded and unloaded proteoliposomes. This efflux shows that [^{14}C]glycine taken up by exchange or unidirectional transport is released in exchange with externally added substrate (results not shown).

The kinetic constants of recombinant purified Hem25p were determined by measuring the initial transport rate at various external [^{14}C]glycine concentrations in the presence of a constant saturating internal concentration (10 mM) of glycine. The K_m and V_{max} values (measured at 25 °C) were 0.75 ± 0.084 mM and 169.8 ± 13.7 nmol/min × mg of protein, respectively (means of 5 experiments). The activity was calculated by taking into account the amount of Hem25p recovered in the proteoliposomes after reconstitution.

Impaired Glycine Uptake in Mitochondria Lacking Hem25p—In other experiments, the uptake of [^{14}C]glycine was measured in proteoliposomes that had been reconstituted with Triton X-100 extracts of mitochondria isolated from wild-type, *hem25*Δ and *hem25*Δ transformed with *HEM25*-pYES2 plasmid (Fig. 2). A very low glycine/glycine exchange activity was observed upon reconstitution of mitochondrial extract from the knock-out strain. This activity was more than double in mitochondria extracts from wild-type and was considerable even in mitochondrial extracts from *HEM25*-pYES2 (Fig. 2). As a control, the [^{14}C]malate/phosphate exchange (the defining reaction of the dicarboxylate carrier, known as Dic1) (23) was virtually the same for all types of reconstituted mitochondrial extracts (Fig. 2). Therefore, the absence of *HEM25* does not affect the expression or the activity of other mitochondrial carriers.

Subcellular Localization of Hem25p—Given that some mitochondrial carrier members are localized in non-mitochondrial membrane (24), the intracellular localization of the recombinant Hem25p was investigated (Fig. 3). Hem25p-expressing cells exhibited green fluorescence (Fig. 3, *A*, *E*, and *I*). Upon staining with MitoTracker Red (mitochondrial specific dye) (Fig. 3*B*), FM4–64 (vacuolar specific dye) (Fig. 3*F*), and DAPI (nucleic acid dye) (Fig. 3*L*), the same cells showed a pattern of fluorescence that merged only with the mitochondrial network (Fig. 3*C*). From the overlapping images it is clear that recombinant Hem25p was localized to mitochondria (Fig. 3*C*). Structural integrity of the cells was documented by phase contrast microscopy (Fig. 3, *D*, *H*, and *N*).

*Growth Characteristics of Wild-type and hem25*Δ—The effect of deletion of the *HEM25* gene on yeast cells was investigated. On YP and SM media supplemented with glucose, *hem25*Δ exhibited a slight but definite growth defect as com-

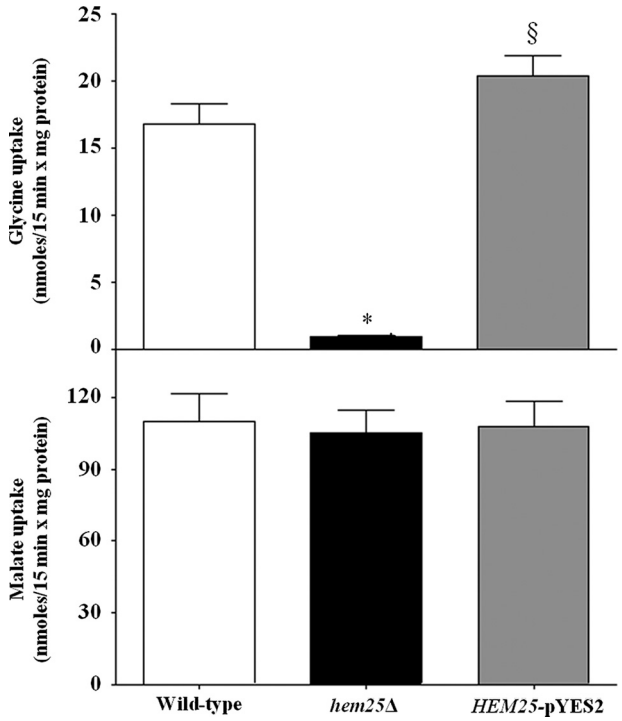

FIGURE 2. **Glycine exchange activities in proteoliposomes reconstituted with mitochondrial extracts.** The mitochondrial extracts (30 μg of protein) from the wild-type (*open bars*), *hem25*Δ (*solid bars*), and *hem25*Δ strains transformed with *HEM25*-pYES2 plasmid (*gray bars*) were reconstituted into liposomes preloaded with 10 mM glycine or 20 mM phosphate. Transport was started by adding 0.75 mM [^{14}C]glycine or 0.1 mM [^{14}C]malate, respectively, and terminated after 15 min. The [^{14}C]malate/phosphate exchange, the defining reaction of the dicarboxylate carrier, was used as control. *, $p < 0.001$ *versus* wild-type cells; §, $p < 0.001$ *versus hem25*Δ cells.

pared with wild-type cells (Fig. 4, *A–D*). However, *hem25*Δ displayed a growth delay in the YP medium supplemented with ethanol (Fig. 4, *E* and *F*). In the SM medium, growth of *hem25*Δ cells on ethanol was very poor after 70 h (Fig. 4, *G* and *H*); in addition, a slower lag-phase of growth was observed more in the SM medium than in the YP medium (Fig. 4*H*). The growth phenotype of *hem25*Δ cells was restored when these cells were transformed with *HEM25*-pYES2, demonstrating that the impaired phenotype is the result of the absence of *HEM25* and not of a secondary effect. The observed defect can also be rescued by supplementation of the SM medium with 10 mM ALA (Fig. 4*G*), whereas the addition of glycine at a high concentration (10 mM) did not restore their lack of growth (Fig. 4*G*). All together, these results indicate that the defect of *hem25*Δ cells to grow on non-fermentable carbon source is overcome by expression of Hem25p in mitochondria or by supplementation of ALA, indicating that the defect is related to glycine transport. Importantly, Fig. 4*G* shows that the *hem25*Δ cell transformed with plasmid carrying the human *SLC25A38* gene restored growth of the *hem25*Δ strain on ethanol. Furthermore, SLC25A38, expressed in *E. coli* and reconstituted in liposomes, shows a significant transport of glycine demonstrating without a doubt that it is the human ortholog of Hem25p and than the human mitochondrial GlyC (Fig. 5).

Hem25p Is Required for the Entry of Glycine into Mitochondria—To confirm the transport function of Hem25p *in vivo*, we investigated the effect of *HEM25* deletion on glycine content in the cellular lysates and mitochondrial extracts from wild-type cells, *hem25*Δ cells, and *hem25*Δ cells transformed with the *HEM25*-pYES2 plasmid grown on ethanol-supplemented medium. GC-MS/MS analysis revealed that in mitochondria isolated from *HEM25*-pYES2 cells the amount of glycine is comparable with that determined in wild-type cells (3.21 ± 0.24 nmol/mg of protein and 2.17 ± 0.15 nmol/mg of protein, respectively) (Fig. 6). On the other hand, *hem25*Δ cells revealed a ~70% decrease of intramitochondrial glycine (0.64 ± 0.034 nmol/mg of protein). In agreement with Guernsey *et al.* (13), no reduction was documented in the amount of total cellular glycine between wild-type (220 ng/10^7 cells) and *hem25*Δ (251 ng/10^7 cells) strains. Furthermore, the level of mitochondrial ALA was also measured and, again, in agreement with Guernsey *et al.* (13), the amount of mitochondrial ALA in the *hem25*Δ strain was reduced compared with control (0.04 nmol/mg of protein *versus* 0.4 nmol/mg of protein), highlighting that loss of Hem25p impairs ALA biosynthesis *in vivo*. ALA was reinstated in the wild-type levels when the mutant was complemented with the missing gene (0.5 nmol/mg of protein) (Fig. 6).

Hem25p and GlyC Deficiency Cause Defects in Respiratory Chain Components—The involvement of Hem25p in heme synthesis implies that the products of the heme pathway could be altered. One of these is heme *b*, which is incorporated into complexes II and III of the respiratory chain and is present in cytochrome *c* (25). Fig. 7 shows immunoblotting of mitochondrial extracts from wild-type, *hem25*Δ, *HEM25*-pYES2, and SLC25A38-pYES2 cells. In the *hem25*Δ lysates we observed a reduction of ~80% of cytochrome *b* protein (Cyt *b*) (Fig. 7*A*, *lane 2*) compared with the wild-type, *HEM25*-pYES2, and SLC25A38-pYES2 strains (Fig. 7*A*, *lanes 1*, *3*, and *4*). Cyt *b* is part of the catalytic core of cytochrome bc_1 complex together with cytochrome c_1 (Cyt c_1) and Rieske iron-sulfur protein (Rip 1) (26). Furthermore, Cyt c_1 forms a subcomplex with the two core proteins Cor1 and Cor2 (27). A Western blot analysis using specific antibodies against Cyt c_1 (Fig. 7*B*) and the Cor1 and Cor2 proteins (Fig. 7*C*) shows that the expression of Cyt c_1 and Cor1 and Cor2 proteins were also markedly decreased only in the *hem25*Δ cells (Fig. 7, *B* and *C*, *lane 2*). To exclude the possibility of a disturbance of the overall protein content by Hem25p, we immunodetected wild-type, *hem25*Δ, *HEM25*-pYES2, and SLC25A38-pYES2 mitochondrial lysates with polyclonal antisera directed against yeast Dic1 (23). In all samples, Dic1 was present in equal amounts (Fig. 7*D*, *lanes 1–4*).

We also measured the heme content in mitochondria isolated from wild-type, *hem25*Δ, *HEM25*-pYES2, and SLC25A38-pYES2 cells; the corresponding results of the spectrophotometric analysis are shown in Fig. 8*A*. A significant decrease of the total level of heme is evident only in the deleted strain as confirmed by fluorescence spectra shown in supplemental Fig. S1. Taken together, these results indicate that the activity of the Hem25p and GlyC carriers is correlated to the mitochondrial heme concentration and the expression of some protein components of yeast cytochrome bc_1 complex.

To further confirm these results, we assayed cytochrome aa_3, *b*-type ($b_{II} + b_H + b_L$), and *c*-type ($c + c_1$) content in mitochondria isolated from the wild-type, *hem25*Δ, *HEM25*-pYES2, and

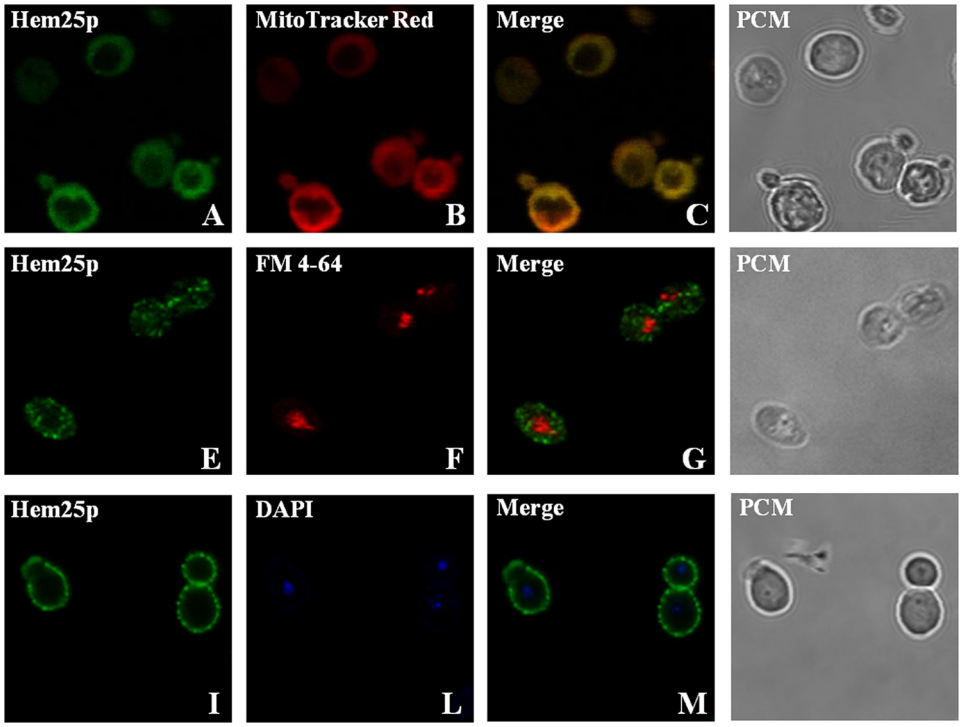

FIGURE 3. **Subcellular localization of recombinant Hem25p after expression in *S. cerevisiae* cells.** *hem25*Δ cells overexpressing the Hem25p/V5 protein were grown as described under "Experimental Procedures." Staining of the Hem25p/V5 protein was performed with mouse anti-V5 monoclonal antibody and anti-mouse antibody with conjugated FITC (*A*, *E*, and *I*). MitoTracker Red (*B*), FM 4-64 (*F*), and DAPI (*L*) were used to locate mitochondria, vacuoles, and nucleic acid in the cells, respectively. Colocalization of the Hem25p/V5 protein and mitochondria are seen as yellow fluorescence in the red and green merged image (*C*). Phase contrast microscopy (*PCM*) was used to monitor the integrity of the cells (*D*, *H*, and *N*). The same cells were photographed first with a FITC-green filter set and then with the MitoTracker or FM 4-64 red filter set or with the DAPI blue filter set. Identical fields are presented in *panels A--D*, *E–H*, or *I–N*.

SLC25A38-pYES2 cells. To perform an absolute determination of the respiratory cytochromes, we calculated nanomoles of each cytochrome type per milligram of mitochondrial protein from different absorbance spectra (experimental data are reported in Fig. 8*B*). The *hem25*Δ strain displayed a marked decrease in mitochondrial cytochromes compared with control, proving once again that the Hem25p and GlyC carriers are relevant for glycine transport into mitochondria, for subsequent mitochondrial synthesis of the heme group, and therefore for respiratory cytochromes. Furthermore, cytochromes were reinstated to the wild-type levels when the mutant was complemented with the *HEM25* or *SLC25A38* genes (Fig. 8*B*).

Respiratory Analysis of Isolated Mitochondria—To better characterize the effects of altered mitochondrial heme content on the oxidative properties of yeast cells, we analyzed the respiratory efficiency of mitochondria freshly isolated from wild-type, *hem25*Δ, *HEM25*-pYES2, and SLC25A38-pYES2 cells grown on SM medium supplemented with ethanol. As shown in Fig. 9, the addition of 5 mM succinate to mitochondria isolated from wild-type cells promoted significant oxygen consumption corresponding to 36 nmol $\times$ ml^{-1} $\times$ min^{-1}/mg of protein. This rate, indicated as V_4, corresponds to the so-called resting state of mitochondrial respiration (respiration state 4). The subsequent addition of 0.2 mM ADP doubled the oxygen consumption rate in wild-type mitochondria (77 nmol O_2 $\times$ ml^{-1} $\times$ min^{-1}/mg of protein). This rate, indicated as V_3, corresponds to the active state of mitochondrial respiration (respiration state 3). In mitochondria isolated from *hem25*Δ cells, a significant reduction in state 4 and state 3 oxygen consumption (V_4 = 11 nmol O_2 $\times$ ml^{-1} $\times$ min^{-1}/mg of protein and V_3 = 21.5 nmol O_2 $\times$ ml^{-1} $-$ min^{-1}/mg of protein, respectively) was found when compared with wild-type. When this respiratory defect was rescued in *hem25*Δ transformed with *HEM25*-pYES2 or SLC25A38-pYES2, the V_3 values were 70 or 81 nmol of O_2 $\times$ ml^{-1} $\times$ min^{-1}/mg of protein, respectively, whereas V_4 values were 34 or 43 nmol of O_2 $\times$ ml^{-1} $\times$ min^{-1}/mg of protein, respectively (Fig. 9). However, no significant variation was observed in respiratory control ratio values (calculated ratio between V_3 and V_4) among the different samples of mitochondria suggesting on the one hand, a good coupling between respiration and phosphorylation and, on the other hand, well preserved integrity of the organelles (28). In a more selective approach we assayed the activity of cytochrome bc_1 complex (29). A significant decrease of activity was only found in mitochondria isolated from *hem25*Δ cells (2.78 $\pm$ 0.19 μmol/min $\times$ mg of protein) with respect to wild-type (12.03 $\pm$ 1.05 μmol/min $\times$ mg of protein).

Discussion

Glycine is an important amino acid for protein synthesis and is a product of one-carbon metabolism as well as a source of one-carbon units. When yeast cells are grown on glucose as the carbon source, glycine can also be produced by the catabolism of threonine in the cytosolic L-threonine aldolase reaction (30). When cells are grown on a non-fermentable carbon source, such as ethanol, glycine is produced from glyoxylate by the alanine-glyoxylate aminotransferase 1 enzyme (31). Furthermore, in *S. cerevisiae* glycine can be catabolized or synthesized in the

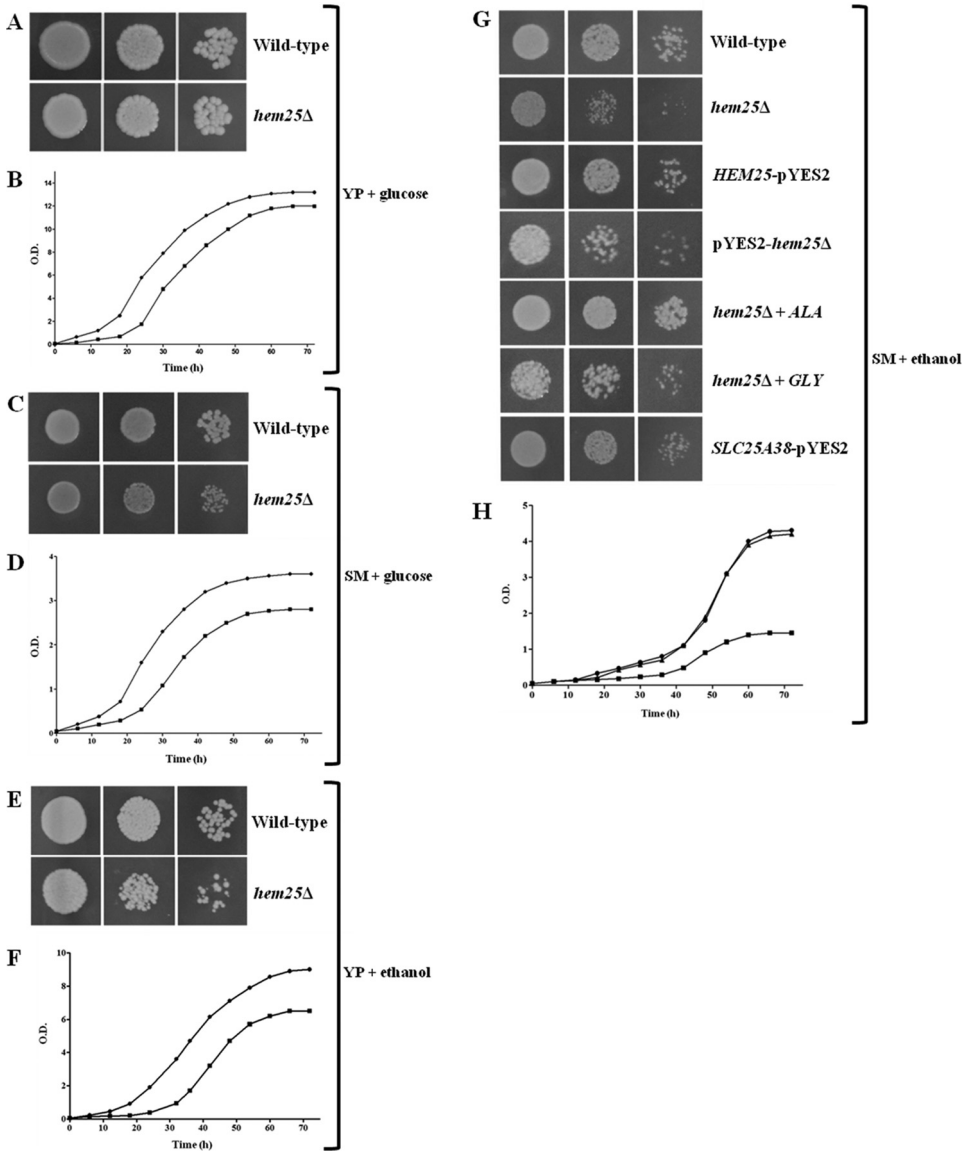

FIGURE 4. **Growth behavior of wild-type and mutant strains under various conditions.** Three-fold serial dilutions of wild-type and *hem25*Δ cells were plated on solid YP medium supplemented with glucose (*A*) or ethanol (*E*) and solid SM medium supplemented with glucose (*C*) or ethanol (*G*). *hem25*Δ cells were also spotted on solid ethanol-supplemented SM medium in the presence of 10 mM *ALA* or 10 mM glycine (*G*). Wild-type and *hem25*Δ cells were inoculated in liquid glucose-supplemented YP (*B*), glucose-supplemented SM (*D*), ethanol-supplemented YP (*F*), or ethanol-supplemented SM medium (*H*). *hem25*Δ cells transformed with the *HEM25*-pYES2 plasmid were spotted (*G*) or inoculated (*H*) on ethanol-supplemented SM medium. *hem25*Δ cells transformed with the *SLC25A38*-pYES2 plasmid were also plated on ethanol-supplemented SM medium (*G*).The optical density (*O.D.*) values at 600 nm given in *B*, *D*, *F*, and *H* refer to cell cultures after the indicated growth times. *Solid circle*, wild-type; *solid square*, *hem25*Δ; *solid triangle*, *hem25*Δ + *HEM25*-pYES2.

reactions of serine hydroxymethyltransferase (Shm1p and Shm2p) isoenzymes (32). The cytoplasmic isozyme Shm2p is the major contributor of one-carbon units and glycine via the breakdown of serine, whereas mitochondrial Shm1p functions preferentially in the direction of L-serine synthesis consuming glycine and one-carbon units (33). The formation of glycine could also be made possible through the glycine cleavage system, which however does not have a crucial role in glycine biosynthesis (34). As glycine is produced mainly in the cytosol by threonine aldolase (encoded by GLY1) (30), a primary function of Hem25p is to catalyze the uptake of glycine into mitochondria, where it is required for heme and protein synthesis. It is also required for the enzymatic activity of glycine cleavage T-protein, a folate-dependent enzyme of the glycine cleavage multienzyme complex that mediates the entry of one-carbon units from glycine into folate-dependent pathways (35).

The results of this study including the transport properties and kinetic characteristics of recombinant Hem25p (encoded by the yeast *YDL119c* gene, also known as HEM25) expressed in *E. coli* and reconstituted into liposomes together with the localization of Hem25p to mitochondria demonstrate that this protein is the mitochondrial transporter for glycine with a very narrow substrate specificity confined to glycine.

To our knowledge, Hem25p is the first mitochondrial protein shown to be capable of transporting glycine, and it is the first time that the mitochondrial carrier for glycine has been identified from any organism through a biochemical characterization. In the past, only one study has provided evidence for the

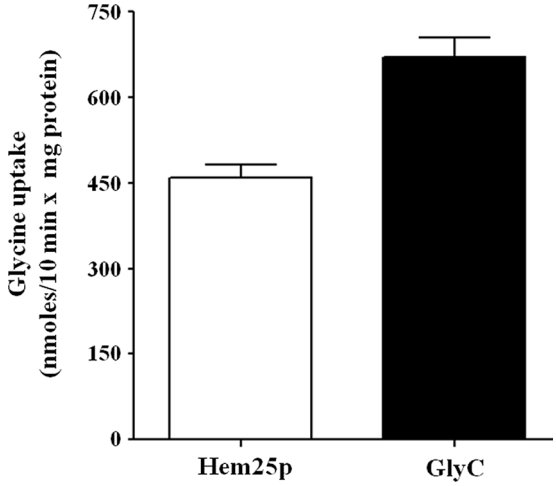

FIGURE 5. **Glycine uptake in proteoliposomes reconstituted with recombinant Hem25p or GlyC.** [^{14}C]glycine (0.75 mM) was added to proteoliposomes reconstituted with Hem25p (*open bar*) or GlyC (*solid bar*) containing 10 mM glycine. The exchange rate was measured after 10 min. Data are the means ± S.D. of at least five independent experiments.

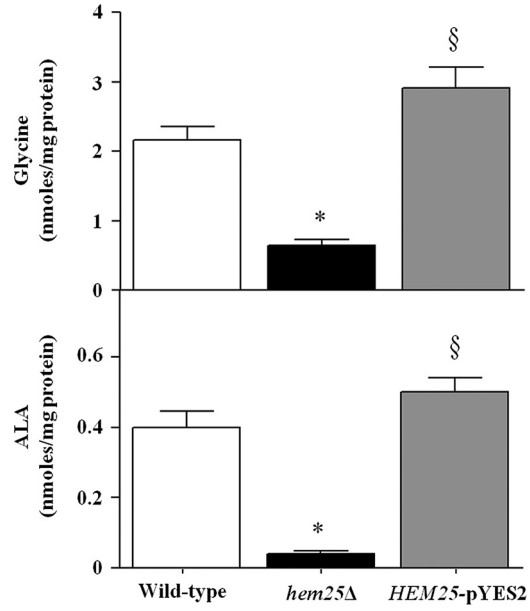

FIGURE 6. **Quantification of glycine and ALA levels in mitochondria extracts by GC-MS/MS analysis.** Mitochondria were extracted from wild-type (*open bars*), *hem25*Δ (*solid bars*), and *hem25*Δ strains transformed with the *HEM25*-pYES2 plasmid (*gray bars*). Data represent the means ± S.D. of at least five independent experiments. *, $p < 0.001$ *versus* wild-type cells; §, $p < 0.001$ *versus hem25*Δ cells.

existence of a glycine-transporting system into rat brain and liver mitochondria, where exogenous glycine was taken up by isolated mitochondria through respiratory-independent, carrier-mediated transport (36). Hem25p does not show significant sequence homology with any other mitochondrial carrier functionally identified until now in yeast, mammals, and plants (15, 37). However, several protein sequences available in databases show a significant homology (~30% amino acid identity) with Hem25p and are orthologs of this transporter in other organisms. These sequences include SLC25A38 from *Homo sapiens* and slc25a38a and slc25a38b from *Danio rerio*. In the SLC25 family no other member is particularly closely related to SLC25A38 (13, 15).

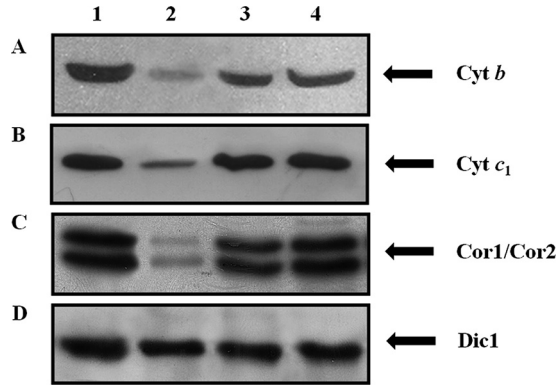

FIGURE 7. **Hem25p deficiency impairs the expression of cytochrome bc_1 complex as evaluated by specific antibodies for cytochrome *b*, cytochrome c_1, Cor1, and Cor2.** Mitochondria (30 μg of protein) were extracted from wild-type (*lane 1*), *hem25*Δ (*lane 2*), *HEM25*-pYES2 (*lane 3*), and *SLC25A38*-pYES2 (*lane 4*) and separated by SDS-PAGE, transferred to nitrocellulose, and immunodetected with antibodies directed against the Cyt *b* (*A*), Cyt c_1 (*B*), Cor1 and Cor2 (*C*), and Dic1 (*D*) proteins. Anti-Dic1 was used as the control.

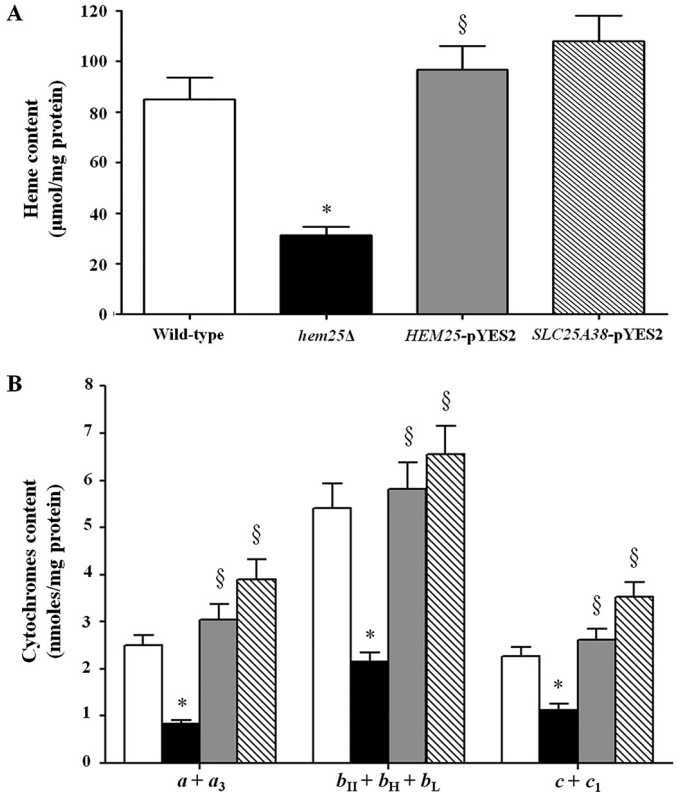

FIGURE 8. **Hem25p deficiency influences mitochondrial content of heme and cytochromes.** Mitochondrial heme level (*A*) and cytochrome aa_3, *b*-type, and *c*-type content (*B*) were measured by spectrophotometry in mitochondria extracted from the wild-type (*open bars*), *hem25*Δ (*solid bars*), and *hem25*Δ strain transformed with the *HEM25*-pYES2 plasmid (*gray bars*) or with *SLC25A38*-pYES2 plasmid (*hatched bars*). Data represent the means ± S.D. of at least five independent experiments. *, $p < 0.005$ *versus* wild-type cells; §, $p < 0.005$ *versus hem25*Δ cells.

Our data support Hem25p and human recombinant GlyC (encoded by the human *SLC25A38* gene) controlling the uptake of glycine into mitochondria based on three relevant suppositions. First, mitochondria from *hem25*Δ cells exhibit a lower level of glycine and a decreased amount of ALA, a precursor of heme because of condensation between glycine and succinyl-

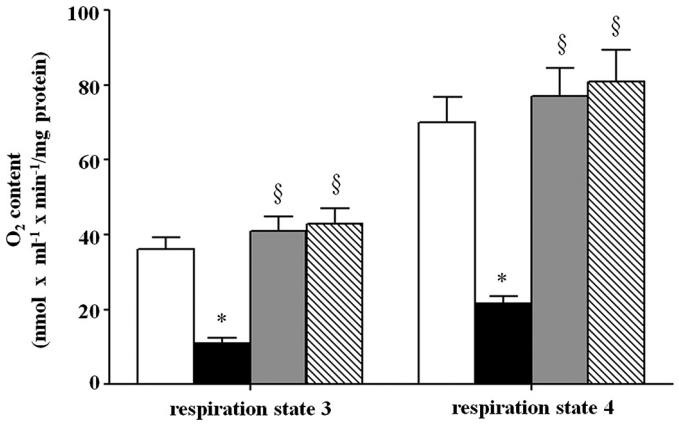

FIGURE 9. **Respiratory efficiency of freshly isolated mitochondria by oxygraphic "Experimental Procedures."** Mitochondria isolated from wild-type (*open bars*), *hem25*Δ (*solid bars*), and *hem25*Δ cells transformed with the *HEM25*-pYES2 plasmid (*gray bars*) or with *SLC25A38*-pYES2 plasmid (*hatched bars*) were grown on SM medium supplemented with ethanol. The rate of oxygen uptake in the presence of added ADP (respiration states 3) and the rate observed when added ADP had been completely phosphorylated to ATP (respiration state 4) were measured by means of a Clark oxygen electrode at 30 °C. The rate of oxygen uptake by yeast mitochondria was expressed as nmol of $O_2 \times ml^{-1} \times min^{-1}$/mg of protein. Data represent the means ± S.D. of at least five independent experiments. *, $p < 0.001$ *versus* wild-type cells; §, $p < 0.001$ *versus hem*Δ cells.

CoA. The normal intramitochondrial levels of glycine in *S. cerevisiae* are restored by complementation of *hem25*Δ cells with the missing gene. The levels of other amino acids did not differ significantly between wild-type and *hem25*Δ yeast cells (*i.e.* the amount of mitochondrial serine was 16.5 nmol/mg of protein and 18.6 nmol/mg of protein for wild-type and the *hem25*Δ strain, respectively). Furthermore, ALAS2 activity, dependent on the PLP enzyme, was assayed in samples of mitochondria purified from the wild-type and knock-out strains. We found no difference in ALAS2 activity between the wild-type (26.29 ± 1.51 nmol/mg × 1 h) and *hem25*Δ (25.54 ± 1.29 nmol/mg × 1 h) strain, confirming that the reduced amount of ALA was exclusively because of the impaired transport of glycine in mitochondria. Furthermore, glycine uptake was strongly reduced in reconstituted *hem25*Δ mitochondrial extract (0.95 ± 0.06 nmol/15 min × mg of protein) compared with wild-type (16.83 ± 1.50 nmol/15 min × mg of protein). This finding is not unrealistic, because many mitochondrial carriers display some overlap of substrate specificity, albeit with lower efficiency, and play different metabolic roles (38). Recently, it has been proposed that Ymc1p is a secondary mitochondrial glycine transporter, because the *hem25*Δ*ymc1*Δ double mutant presented a lower level of heme content compared with the single *hem25*Δ or *ymc1*Δ mutant (14); however, data in the literature pointed out a role for *YMC1* in carbon source utilization (39, 40). Trotter *et al.* (39) found a relationship between *YMC1*, its paralog *YMC2*, and the mitochondrial 2-oxodicarboxylate transporters, Odc1p and Odc2p. In fact, *YMC1* and *YMC2* are involved in oleic acid and glycerol utilization (39). They are able to suppress the *odc1*Δ*odc2*Δ growth phenotype on oleic acid medium (39). Their mRNAs increase in the presence of oleic acid or glycerol, as compared with glucose, and the deletion of all four transporters (*ymc1*Δ*ymc2*Δ, *odc1*Δ*odc2*Δ) prevents growth on oleic acid as a sole carbon source (39). Moreover, Dallabona *et al.* (40) demonstrate that only *YMC1* and *ODC1* are able to suppress the *sym1*Δ phenotype, which is probably due to a defective anaplerotic flux of tricarboxylic acid (TCA) cycle intermediates (40). They supposed that Odc1p and Ymc1p play an anaplerotic role in the TCA cycle by transferring intermediates from peroxisomes to mitochondria, thus contributing to the utilization of energy substrates (*e.g.* long chain fatty acids) (40).

Second, the *hem25*Δ strain exhibits growth delay only on SM medium supplemented with non-fermentable carbon sources. Likewise, the *hem25*Δ mutant grows normally when complemented with Hem25p. The growth is also restored by the addition of ALA, the first mitochondrial intermediate in heme synthesis. The uptake of glycine is required in mitochondria also for the synthesis of ALA. Thus, the simplest explanation for the growth phenotype of the *hem25*Δ mutant is that it is caused mainly by insufficient synthesis of ALA and that it is rescued by its addition. On the contrary, the addition of exogenous glycine is only insufficient to restore the growth of *hem25*Δ cells and the normal level of mitochondrial heme. These results highlight that Hem25p is the main mitochondrial glycine carrier involved in heme synthesis. Furthermore, we show that the human recombinant GlyC reconstituted in liposomes is able to transport glycine and that its corresponding gene fully restores the growth defect of the *hem25*Δ strain.

Last, a reduced amount of mitochondrial ALA is the cause of a reduced level of heme. Different forms of heme are contained in cytochromes and oxidative phosphorylation complexes (25, 41). We found that in the *hem25*Δ mutant the expression and activity of the yeast cytochrome bc_1 complex is impaired. Consequently, in mitochondria isolated from *hem25*Δ cells a significant reduction in state 4 and state 3 oxygen consumption is evident when compared with wild-type cells. However, if the mutant is complemented with the yeast or human missing genes the observed defects are rescued.

Taken together, our results on the phenotypic analysis of the *hem25*Δ mutant on non-fermentative substrates suggest that in mitochondria Hem25p plays an important role in the life of the cell (*i.e.* heme synthesis) and for respiratory growth (expression and function of some components of the respiratory chain). The fact that human GlyC is able to transport glycine and complements defective mitochondrial glycine transport in the *hem25*Δ strain demonstrate that human *SLC25A38* has the same function as *HEM25* in yeast (Fig. 10). The present results provide novel insights into the biochemical characterization and molecular mechanisms involved in mitochondrial glycine transport and may offer new avenues to develop innovative therapies for *SLC25A38*-related disorders.

Experimental Procedures

Yeast Strains and Growth Conditions—BY4742 wild-type (MATα, *his3*Δ1, *leu2*Δ0, *lys2*Δ0, *ura3*Δ0) and *hem25*Δ yeast strains were provided by the EUROFAN resource center EUROSCARF (Frankfurt, Germany). The *YDL119c* locus of the *S. cerevisiae* BY4742 strain was replaced by kanMX4 (42). All the yeast strains were grown in YP containing 2% (w/v) bactopeptone and 1% (w/v) yeast extract at pH 4.8 or in synthetic complete medium (0.67% w/v yeast nitrogen base (Difco), 0.1%

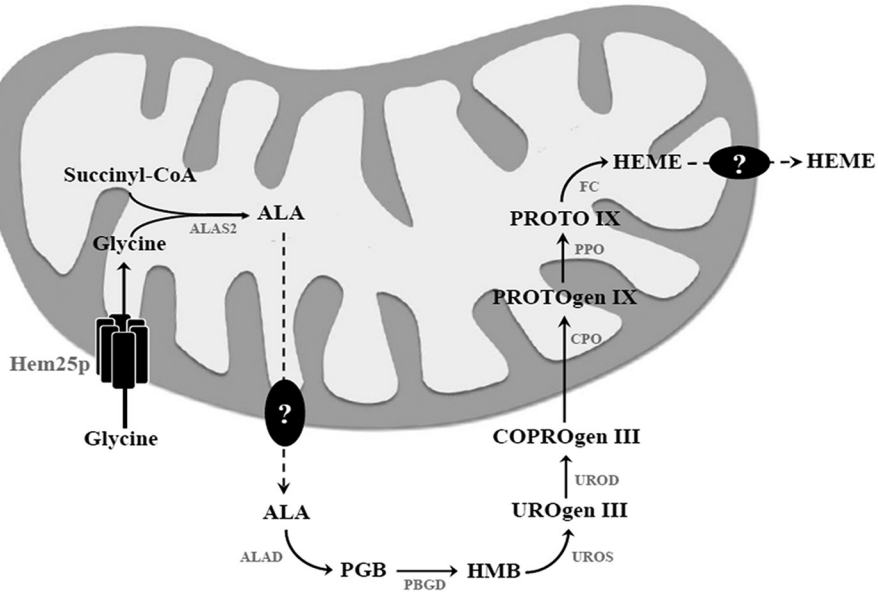

FIGURE 10. **Scheme showing metabolic compartmentalization and the role of mitochondrial Hem25p in heme biosynthesis.** Heme biosynthesis is initiated in mitochondria with the condensation of glycine and succinyl-CoA to ALA by ALAS2. ALA is subsequently exported into the cytosol where it is condensed to porphobilinogen (PBG) by ALA dehydratase (*ALAD*). Four molecules of porphobilinogen are subsequently used to form the unstable hydroxymethylbilane (*HMB*) by porphobilinogen deaminase (*PBGD*) followed by the cyclization to uroporphyrinogen III (*UROgen III*) by uroporphyrinogen III synthase (*UROS*). Uroporphyrinogen III is decarboxylated by UROgen III decarboxylase (*UROD*) to coproporphyrinogen III (*COPROgen III*), which in turn is redirected to mitochondria where heme biosynthesis carries on by coproporphyrinogen III oxidase (*CPO*) with the formation of protoporphyrinogen IX (*PROTOgen IX*). Next, protoporphyrinogen oxidase (*PPO*) forms protoporphyrin IX (*PROTO IX*). The final product, heme, is formed by ferrochelatase (*FC*), which mediates the insertion of ferrous iron in PROTO IX. The intermediates ALA and COPROgen III and the substrate glycine need to be transported across mitochondrial membranes. Hem25p (such as its human orthologue GlyC) is the mitochondrial carrier for glycine. The *question mark* indicates a still unknown transporter that catalyzes the exit of ALA from mitochondria.

w/v drop-out mix), or in SM medium (0.67% w/v yeast nitrogen base and essential amino acids) at 30 °C (43). All media were supplemented with a fermentable (2% w/v glucose) or a non-fermentable (3% w/v glycerol or 2% w/v ethanol) carbon source.

Construction of Expression Plasmids—The coding sequences of the yeast *HEM25* and human orthologue *SLC25A38* were cloned into the pET21b vector for expression in *E. coli*. The *HEM25* open reading frame was amplified from *S. cerevisiae* genomic DNA by PCR using primers corresponding to the extremities of the coding sequences with additional NdeI and HindIII sites (5′-AAGCTTCATATGACTGAGCAAGCAACTAA-3′ as the forward primer and 5′-GAATTCAAGCTTGAATCTTTTGACCAACTCCT-3′ as the reverse primer, respectively). The coding sequence of the human *SLC25A38* gene was obtained by RT-PCR reaction using total RNA extracted from HepG2 cells as template (44, 45) and the primers with additional NdeI and HindIII sites (5′-AAGCTTCATATGATTCAGAACTCACGTCC-3′ and 5′-GAATTCAAGCTTGGACTTCAGGCCCATCTTGG-3′, respectively). The amplified products were cloned into the NdeI-HindIII sites of the expression vector pET21b that had been previously modified by cloning into HindIII-XhoI sites a cDNA sequence coding for a V5 epitope followed by six histidines (46).

The *HEM25*-pYES2 and *SLC25A38*-pYES2 plasmids were constructed by cloning the coding sequences of *HEM25* and *SLC25A38*, respectively, into the yeast pYES2 expression vector. To create the *HEM25*-pYES2, the *HEM25* cDNA was amplified by PCR using the *HEM25*-pET21b construct as template. The forward and reverse primers (5′-AAGCTTGGATCCACCATGACTGAGCAAGCAACTAA-3′ and 5′-AAGCTTCTCGAGTTACGTAGAATCGAGACCGAGGAG-3′, respectively) carried BamHI and XhoI restriction sites, respectively, as linkers. The reverse primer also carried a cDNA sequence coding for a V5 epitope. Similarly, to generate the *SLC25A38*-pYES2 construct, the coding sequence of *SLC25A38* was obtained by PCR using *SLC25A38*-pET21b as template and the primers with additional BamHI and XhoI sites (5′-AAGCTTGGATCCACCATGATTCAGAACTCACGTCC-3′ and 5′-AAGCTTCTCGAGTTACGTAGAATCGAGACCGAGGAG-3′, respectively).

The pET21b and pYES2 vectors, prepared as above, were transformed into *E. coli* DH5α cells. Transformants were selected on ampicillin (100 μg/ml) and screened by direct colony PCR and by restriction digestion of purified plasmids. The sequences of the inserts were verified.

Bacterial Expression and Purification of Recombinant Proteins—The overexpression of Hem25p and GlyC as inclusion bodies in the cytosol of *E. coli* BL21(DE3) was accomplished as described previously (47). Control cultures with the empty vector were processed in parallel. Inclusion bodies were purified on sucrose density gradient and washed at 4 °C, first with TE buffer (10 mM Tris/HCl, 1 mM EDTA, pH 8), then twice with a buffer containing Triton X-114 (2% w/v) and 10 mM HEPES, pH 8, and, finally, with HEPES 10 mM, pH 7.5 (48). Proteins were solubilized in 2% (w/v) Sarkosyl® and purified by centrifugation and Ni^{2+}-nitrilotriacetic acid-agarose affinity chromatography, as described previously (49).

Reconstitution into Liposomes and Glycine Transport Assays—The recombinant proteins in Sarkosyl® (*N*-dodecanoyl-*N*-methyl-glycine sodium salt) were reconstituted into liposomes in the presence or absence of substrates (50). The

reconstitution mixture contained purified proteins (100 μl with 0.5–1 μg of protein), 10% (w/v) Triton X-114 (90 μl), 10% (w/v) phospholipids as sonicated liposomes (90 μl), 10 mM glycine (except where otherwise indicated), 20 mM HEPES at pH 7.5 (except where otherwise indicated), and water to a final volume of 700 μl. These components were mixed thoroughly, and the mixture was recycled 13 times through the same Amberlite column (Bio-Rad).

External substrate was removed from proteoliposomes on Sephadex G-75 columns, pre-equilibrated with 50 mM NaCl, 10 mM HEPES at pH 7.5 (except where otherwise indicated) (47). Transport at 25 °C was started by adding, at the indicated concentrations, L-[^{14}C]glycine (Scopus Research BV, The Netherlands) to substrate-loaded proteoliposomes (exchange) or to empty proteoliposomes (uniport). In both cases, transport was terminated by adding of 30 mM PLP and 10 mM bathophenanthroline, which in combination and at high concentrations completely inhibit the activity of several mitochondrial carriers (50).

In control samples, the inhibitors were added at time 0 together with the radioactive substrate according to the "inhibitor stop method" (18). Finally, the external substrate was removed by a Sephadex G-75 column, and the radioactivity in the liposomes was measured. The experimental values were corrected by subtracting control values. The initial transport rate was calculated from the radioactivity taken up by proteoliposomes after 1 min (in the initial linear range of substrate uptake).

Overexpression in S. cerevisiae—The resulting yeast expression plasmids were introduced in the deleted strain, and transformants were selected on synthetic complete medium agar plates without uracil, supplemented with 2% (w/v) glucose, precultured on synthetic complete medium without uracil supplemented with 2% (w/v) glucose for 14–16 h, diluted to a final A_{600} = 0.05 in YP supplemented with 3% (w/v) glycerol and 0.1% (w/v) glucose, and grown to early-exponential phase. Galactose (0.4% w/v) was added 4 h before harvesting to induce recombinant protein overexpression.

Mitochondria, obtained as described previously by Daum *et al.* (51), were isolated from wild-type, *hem25*Δ, and *HEM25*-pYES2 cells and solubilized in a buffer containing 3% (w/v) Triton X-100, 20 mM NaCl, 10 mM HEPES, pH 7.5, and supplemented with 2 mg/ml cardiolipin at a final concentration of 1.5 mg of protein/ml. After incubation for 20 min at 4 °C, the mixture was centrifuged at 8000 × *g* for 20 min thereby obtaining a supernatant, referred to as mitochondrial extract. The mitochondrial extract was reconstituted by cyclic removal of detergent (49, 52).

Subcellular Localization of Recombinant Proteins—The *hem25*Δ yeast strain was transformed with the pYES2 vector containing the coding sequence for yeast Hem25p/V5 protein. Indirect immunofluorescence experiments were carried out according to Pringle's (53) procedure with some modifications (54). Cells were grown in glycerol-supplemented YP medium until early-logarithmic phase, and the expression of recombinant proteins was induced by adding 0.4% (w/v) galactose for 4 h at 30 °C. Then, formaldehyde solution was added directly to the cells in growth medium to a final concentration of 3.7% (w/v). After 1 h at 30 °C, the cells were pelleted by centrifugation at 1301 × *g* for 5 min at room temperature and resuspended in phosphate-buffered paraformaldehyde containing 100 mM potassium phosphate, pH 6.5, 1 mM $MgCl_2$, and 3.7% (w/v) paraformaldehyde. After 16 h at 30 °C, the cells were washed with distilled water and then incubated for 10 min at 30 °C in 1 ml of solution containing 200 mM Tris/HCl, pH 8.0, 1 mM EDTA, and 1% (v/v) β-mercaptoethanol. The pellet was resuspended in 1 ml of zymolyase buffer (1.2 M sorbitol, 20 mM potassium phosphate, 1 mM $MgCl_2$, pH 7.4). Zymolyase-20T (Seikagaku Kogyo Co., Tokyo, Japan) (5 mg/g of cell, wet weight) was added, and the suspension was incubated for 30–60 min at 30 °C with gentle shaking for conversion into spheroplasts. After digestion, cells were spun down at 1301 × *g* and washed once with 1.2 M sorbitol, then resuspended gently and incubated for 2 min in 1.2 M sorbitol and 2% (w/v) SDS. Cells were washed twice with 1.2 M sorbitol. Spheroplasts (20 μl) were incubated for 1 h at 30 °C in the presence of 100 nM MitoTracker Red, 32 nM FM 4-64 Dye (*N*-(3-triethylammoniumpropyl)-4-(6-(4(diethylamino) phenyl) hexatrienyl) pyridinium dibromide) or 1 μg/ml DAPI (4′,6-diamidino-2-phenylindole, dihydrochloride) (Molecular Probes, The Netherlands), washed twice with PBS containing 5 mg/ml BSA (PBS-BSA) before adding a primary antibody against V5 (1 μg/ml in PBS-BSA), and incubated for 1 h at 30 °C. After washing twice for 5 min with PBS-BSA, the secondary antibody anti-mouse FITC-conjugate (Santa Cruz Biotechnology, Inc., CA) was added at 1:100 dilution in PBS-BSA for 1 h at 30 °C. In the final step, the coverslips were washed 3 times in PBS-BSA, and the cells were observed by a confocal laser scanning microscope (LSM 700, Zeiss). Observations were performed as described in De Caroli *et al.* (55).

Sample Preparation for Yeast Metabolite Analysis—A previous procedure for preparation of yeast cell lysates described by Villas-Bôas *et al.* (56) was used. Yeast cultures were grown in overnight shaking in YP media supplemented with 2% (w/v) glucose at 30 °C to A_{600} = 3.5 and then were quenched by quickly adding 10 ml of overnight cultures to 40 ml of chilled methanol-water solution (60% v/v). Cells were harvested for 5 min at 1540 × *g* (0 °C), and the pellets were resuspended in 3 ml of chilled 100% (v/v) methanol. A 1-ml aliquot of this suspension was snap-frozen in liquid nitrogen, thawed in an ice-bath, and centrifuged at 770 × *g* for 20 min (0 °C). The supernatant was collected, and an additional 0.5 ml of chilled 100% (v/v) methanol was added to the pellet and vortexed for 30 s. Suspensions were centrifuged at 770 × *g* for 20 min (0 °C), and both supernatants were pooled. Metabolite extractions were carried out on yeast mitochondria isolated from wild-type, *hem25*Δ, and *HEM25*-pYES2 cells. Yeast mitochondria were obtained as described above.

Glycine and ALA Analysis by Gas Chromatography Coupled to Tandem Mass Spectrometry (GC-MS/MS)—Yeast lysates and mitochondria obtained from wild-type, *hem25*Δ, and *HEM25*-pYES2 cells were centrifuged, and the supernatant was transferred into a glass vial; norleucine (Sigma) was added as the internal standard (10 μl of an 80 ng/μl norleucine solution) and freeze-dried (57, 58). The residue was reconstituted with 200 μl of DMF (*N*,*N*-dimethylformamide) (VWR International

TABLE 1

Overview of the electron impact multiple reaction monitoring GC-MS/MS method and relevant performance characteristics

Rt, retention time; MRM, multiple reaction monitoring transitions (precursor ion, target ion, and optimized collision energy for both Q and qi), limit of detection, limit of quantification, accuracy, repeatability; RSD, relative S.D.

Compound	ALA	Glycine	Norleucine
Rt (min)	18.53	9.84	13.54
MRM transitions/ collision energy			
Quantification (Q)	144 → 73/−18V	218 → 147/−18V	302 → 274/−18V
Confirmation (qi)	302 → 116/−10V	246 → 218/−10V	
Slope (±s)	0.492 (± 0.005)	1.439 (± 0.013)	
Intercept (±s)	−0.006 (± 0.003)	0.010 (± 0.007)	
R2	0.9994	0.9996	
Limit of detection (ng/μl)	0.0415	0.0356	
Limit of quantification (ng/μl)	0.0929	0.0622	
Recovery (%)	94 ± 5	101 ± 3	
Repeatability (RSD)			
Intraday ($n = 3$)	3.2	2.1	
Interday ($n = 5$)	5.8	4.3	

PBI S.r.l., Italy) and 50 μl of MTBSTFA (*N-tert*-butyldimethylsilyl-*N*-methyltrifluoroacetamide) (Sigma) (59). Derivatization with MTBSTFA was performed at 60 °C for 30 min. If not otherwise indicated, samples were placed on the GC-MS/MS autosampler tray immediately after preparation. After cooling the solution at room temperature for 5 min, 1 μl of the solution was injected into the GC-MS/MS. Samples were run on a GC-QqQ-MS (Bruker 456 gas chromatograph coupled to a triple quadrupole mass spectrometer Bruker Scion TQ) equipped with an autosampler (GC PAL, CTC Analytics AG). 1 μl of the sample was injected in split mode (split ratio 5:1). The GC was operated at a constant flow of 1.2 ml/min, and analytes were separated on a Restek Rxi 5Sil MS capillary column (30 m with a 10-m "built-in" guard column, inner diameter 250 μm, and film thickness 0.25 μm). The oven was kept at 130 °C for 2 min after injection, then a temperature gradient of 5 °C/min was employed until 220 °C was reached and then 10 °C/min up to 300 °C. The oven was then held at 300 °C for 10 min.

The total run time was 38 min. The mass detector was operated at 70 eV in the electron impact ionization mode. The ion source and transfer line temperature were 200 °C and 280 °C, respectively. The collision gas was argon. For both ALA and Gly quantification, an MS/MS procedure was employed in multiple reaction monitoring (MRM) mode using argon 99.999% (w/v) (Sapio BIC) as collision gas at a pressure of 1.5147 mbar in the collision cell (data collected in Table 1). To ensure a reliable identification of analytes, two MS/MS transitions were selected within ± 0.2 min of the compounds' retention time. Product ion abundance was maximized by optimal collision energy voltage. The dwell time per transition was 0.1 s. For identity confirmation both the match in retention time and the confirmation ratio (Q/qi), *i.e.* the ratio between the intensity of the quantification (Q) and confirmation (qi) transitions recorded for each compound, were required to confirm positive identification in a sample. Bruker MS Work station 8 application manager was used to process the data. Method validation included determination of linear range, limit of detection, limit of quantification, recovery, and repeatability (Table 1 gives an overview of the relevant data). Linearity was evaluated by least squares regression and expressed as r2. The calibration curve was linear in the investigated range of six concentration levels (0.04, 0.1, 0.2, 0.4, 0.7, and 1.0 ng/μl). Limit of quantification and limit of detection were estimated, respectively, from the calibration curve as the concentration for which there is a 5% chance of having a false-positive and the concentration for which there is a coefficient of variation on the expected value <10%. Experiments to evaluate surrogate or marginal recovery were performed with samples spiked with 100 ng Gly and ALA; the average recoveries were calculated on five different experiments. The repeatability of the present method was estimated during the entire analytical procedure (sample pretreatment, derivatization, and GC/MSMS separation) using standard solutions (0.4 ng/μl ALA; 0.1 ng/μl Gly). The intraday and interday precision values, expressed in terms of relative standard deviation, were assessed by performing an analysis three times on the same day and by conducting the analysis on five different days in one month, respectively.

Determination of Mitochondrial Heme and Cytochrome Content—Mitochondria were isolated from wild-type, *hem25*Δ, *HEM25*-pYES2, and *SLC25A38*-pYES2 cells and solubilized in 1% (w/v) Triton-X100. Heme was quantified by spectrophotometry according to the method of Drabkin with some modifications (60). To determine fluorescence spectra of heme, equal amounts of mitochondrial protein were mixed with 2 mol/liter oxalic acid and heated to 95 °C for 30 min to release iron from heme and generate protoporphyrin IX. Samples were then centrifuged for 10 min at 1000 × *g* at 4 °C to remove debris. The fluorescence intensity of the supernatant was measured with a Jasco FP 750 fluorimeter (Jasco Corp., Tokyo, Japan). The excitation wavelength was 405 nm, and emission was measured at 600 nm. The 662-nm emission peak has lower fluorescence than the peak at 600 nm but also has other interference (61).

Determination of the contents of cytochromes aa_3, *b*-type ($b_{II} + b_H + b_L$) and *c*-type ($c + c_1$) in isolated mitochondria was carried out in 1 ml of respiratory buffer (300 mM sucrose, 1 mM EDTA, 5 mM Mops, 10 mM KH_2PO_4, 2 mM $MgCl_2$, 0.1% (w/v) BSA, and 5 mM succinate, pH 7.4) (62). Individual fully reduced (with excess sodium dithionite) or fully oxidized (with excess ferricyanide) absorbance spectra were recorded between 500 and 650 nm, and the concentration of each type of cytochrome was determined from the difference (reduced-oxidized) spectrum at the maximum absorption value for each one, normalized by the absorbance of the respective isosbestic point. Values were calculated by the Beer-Lambert law, as described previously (62), and expressed relative to protein concentration.

Mitochondrial Respiration Efficiency—Mitochondrial respiration (0.2 mg of mitochondrial protein/ml) was measured in a medium consisting of 300 mM sucrose, 1 mM EDTA, 5 mM Mops, 10 mM KH_2PO_4, 2 mM $MgCl_2$, 0.1% (w/v) BSA, and 5 mM succinate, pH 7.4, by means of a Clark oxygen electrode at 30 °C. After 2 min, state 3 respiration was induced by the addition of 0.2 mM ADP. The rate of oxygen uptake by yeast mitochondria (V) was expressed as nmol of $O_2 \times ml^{-1} \times min^{-1}$/mg of protein. The respiratory control ratio was calculated by dividing V_3 (rate of oxygen uptake measured in the presence of respiratory substrates + ADP, *i.e.* state 3 of respiration or active state of respiration) by V_4 (rate of oxygen uptake measured with

respiratory substrates alone, *i.e.* state 4 of respiration or resting state of respiration) (63). The enzymatic bc_1 complex activity was determined by measuring the reduction of oxidized cytochrome *c* at 550 nm as described previously (26).

Other Methods—Proteins were analyzed by SDS-PAGE and stained with Coomassie Blue dye or transferred to nitrocellulose membranes according to standard procedure. Western blotting was carried out with mouse anti-V5 monoclonal antibody (Sigma) against the expressed proteins in *E. coli*. The amount of proteins incorporated into liposomes was measured as described previously (64) and was proved to be ~20% that of the protein added to the reconstitution mixture.

Moreover mitochondrial proteins were separated by SDS-PAGE, transferred to a nitrocellulose membrane, and analyzed by Western blotting using rabbit antibodies against yeast complex III Cyt *b*, Cyt c_1, or Cor1 and -2 subunits of the respiratory chain prepared in the Trumpower laboratory (27). Antibody against yeast Dic1 was prepared by Abmart. The secondary antibodies were peroxidase-conjugated anti-rabbit IgG or anti-mouse IgG (Santa Cruz Biotechnology, Inc.). The immunoreacted proteins were detected by enhanced chemiluminescence, and the amount of proteins was estimated by laser densitometry of stained samples using carbonic anhydrase as a protein standard.

Author Contributions—L. C. and P. L. conceived the project, designed the experiments, and wrote the manuscript. P. L. performed the biochemical experiments and analyzed the data. F. D. and L. S. designed and performed the molecular biology experiments. G. D. B. and A. P. conceived metabolite analyses by GC-MS/MS. L. M. performed confocal microscopy analysis. E. P. analyzed the yeast phenotype. E. P. and C. M. T. M. assisted in data interpretation. C. M. T. M. and V. D. participated in the discussion of the project and were involved in the revision of the manuscript. L. C. and V. D. directed and supervised the project. All authors read and approved the final manuscript.

Acknowledgment—We especially thank to the PON Cod. 2HE-PONa3_00334 through which a ZEISS LSM700 confocal microscope was purchased.

References

1. Kannengiesser, C., Sanchez, M., Sweeney, M., Hetet, G., Kerr, B., Moran, E., Fuster Soler, J. L., Maloum, K., Matthes, T., Oudot, C., Lascaux, A., Pondarré, C., Sevilla Navarro, J., Vidyatilake, S., Beaumont, C., Grandchamp, B., and May, A. (2011) Missense *SLC25A38* variations play an important role in autosomal recessive inherited sideroblastic anemia. *Haematologica* **96,** 808–813
2. Ponka, P., and Prchal, J. T. (2010) Hereditary and acquired sideroblastic anemias. In *Williams Hematology* (Kaushansky, K., Beutler, E., Seligsohn, U., Lichtman, M. A., Kipps, T. J., and Prchal, J. T., eds.) 8th Ed., pp. 865–881, McGraw Hill, New York
3. Williams, D. M. (1983) Copper deficiency in humans. *Semin. Hematol.* **20,** 118–128
4. Harigae, H., and Furuyama, K. (2010) Hereditary sideroblastic anemia: pathophysiology and gene mutations. *Int. J. Hematol.* **92,** 425–431
5. Camaschella, C. (2009) Hereditary sideroblastic anemias: Pathophysiology, diagnosis, and treatment. *Semin. Hematol.* **46,** 371–377
6. Fleming, M. D. (2011) Congenital sideroblastic anemias: iron and heme lost in mitochondrial translation. *Hematology Am. Soc. Hematol. Educ. Program.* **2011,** 525–531
7. Bergmann, A. K., Campagna, D. R., McLoughlin, E. M., Agarwal, S., Fleming, M. D., Bottomley, S. S., and Neufeld, E. J. (2010) Systematic molecular genetic analysis of congenital sideroblastic anemia: Evidence for genetic heterogeneity and identification of novel mutations. *Pediatr. Blood Cancer* **54,** 273–278
8. Bottomley, S. S., May, B. K., Cox, T. C., Cotter, P. D., and Bishop, D. F. (1995) Molecular defects of erythroid 5-aminolevulinate synthase in X-linked sideroblastic anemia. *J. Bioenerg. Biomembr.* **27,** 161–168
9. Ducamp, S., Schneider-Yin, X., de Rooij, F., Clayton, J., Fratz, E. J., Rudd, A., Ostapowicz, G., Varigos, G., Lefebvre, T., Deybach, J. C., Gouya, L., Wilson, P., Ferreira, G. C., Minder, E. I., and Puy, H. (2013) Molecular and functional analysis of the C-terminal region of human erythroid-specific 5-aminolevulinic synthase associated with X-linked dominant protoporphyria (XLDPP). *Hum. Mol. Genet.* **22,** 1280–1288
10. Cox, T. C., Bottomley, S. S., Wiley, J. S., Bawden, M. J., Matthews, C. S., and May, B. K. (1994) X-linked pyridoxine-responsive sideroblastic anemia due to a Thr-388-to-Ser substitution in erythroid 5-aminolevulinate synthase. *N. Engl. J. Med.* **330,** 675–679
11. Chiabrando, D., Mercurio, S., and Tolosano, E. (2014) Heme and erythropoieis: more than a structural role. *Haematologica* **99,** 973–983
12. Ajioka, R. S., Phillips, J. D., and Kushner, J. P. (2006) Biosynthesis of heme in mammals. *Biochim. Biophys. Acta* **1763,** 723–736
13. Guernsey, D. L., Jiang, H., Campagna, D. R., Evans, S. C., Ferguson, M., Kellogg, M. D., Lachance, M., Matsuoka, M., Nightingale, M., Rideout, A., Saint-Amant, L., Schmidt, P. J., Orr, A., Bottomley, S. S., Fleming, M. D., *et al.* (2009) Mutations in mitochondrial carrier family gene SLC25A38 cause nonsyndromic autosomal recessive congenital sideroblastic anemia. *Nat. Genet.* **41,** 651–653
14. Fernández-Murray, J. P., Prykhozhij, S. V., Dufay, J. N., Steele, S. L., Gaston, D., Nasrallah, G. K., Coombs, A. J., Liwski, R. S., Fernandez, C. V., Berman, J. N., and McMaster, C. R. (2016) Glycine and folate ameliorate models of congenital sideroblastic anemia. *PLoS Genet.* **12,** e1005783
15. Palmieri, F. (2013) The mitochondrial transporter family SLC25: identification, properties, and physiopathology. *Mol. Aspects Med.* **34,** 465–484
16. Kardon, J. R., Yien, Y. Y., Huston, N. C., Branco, D. S., Hildick-Smith, G. J., Rhee, K. Y., Paw, B. H., and Baker, T. A. (2015) Mitochondrial ClpX activates a key enzyme for heme biosynthesis and erythropoiesis. *Cell* **161,** 858–867
17. Agrimi, G., Di Noia, M. A., Marobbio, C. M., Fiermonte, G., Lasorsa, F. M., and Palmieri, F. (2004) Identification of the human mitochondrial *S*-adenosylmethionine transporter: bacterial expression, reconstitution, functional characterization, and tissue distribution. *Biochem. J.* **379,** 183–190
18. Palmieri, F., Indiveri, C., Bisaccia, F., and Iacobazzi, V. (1995) Mitochondrial metabolite carrier proteins: purification, reconstitution, and transport studies. *Methods Enzymol.* **260,** 349–369
19. Fiermonte, G., Dolce, V., and Palmieri, F. (1998) Expression in *Escherichia coli*, functional characterization, and tissue distribution of isoforms A and B of the phosphate carrier from bovine mitochondria. *J. Biol. Chem.* **273,** 22782–22787
20. Iacopetta, D., Madeo, M., Tasco, G., Carrisi, C., Curcio, R., Martello, E., Casadio, R., Capobianco, L., and Dolce, V. (2011) A novel subfamily of mitochondrial dicarboxylate carriers from *Drosophila melanogaster*: biochemical and computational studies. *Biochim. Biophys. Acta* **1807,** 251–261
21. Dolce, V., Cappello, A. R., and Capobianco, L. (2014) Mitochondrial tricarboxylate and dicarboxylate-tricarboxylate carriers: from animals to plants. *IUBMB Life* **66,** 462–471
22. Dolce, V., Scarcia, P., Iacopetta, D., and Palmieri, F. (2005) A fourth ADP/ATP carrier isoform in man: identification, bacterial expression, functional characterization, and tissue distribution. *FEBS Lett.* **579,** 633–637
23. Palmieri, L., Vozza, A., Hönlinger, A., Dietmeier, K., Palmisano, A., Zara, V., and Palmieri, F. (1999) The mitochondrial dicarboxylate carrier is essential for the growth of *Saccharomyces cerevisiae* on ethanol or acetate as the sole carbon source. *Mol. Microbiol.* **31,** 569–577
24. Palmieri, L., Rottensteiner, H., Girzalsky, W., Scarcia, P., Palmieri, F., and Erdmann, R. (2001) Identification and functional reconstitution of the yeast peroxisomal adenine nucleotide transporter. *EMBO J.* **20,** 5049–5059

25. Kim, H. J., Khalimonchuk, O., Smith, P. M., and Winge, D. R. (2012) Structure, function, and assembly of heme centers in mitochondrial respiratory complexes. *Biochim. Biophys. Acta* **1823,** 1604–1616
26. Conte, A., Papa, B., Ferramosca, A., and Zara, V. (2015) The dimerization of the yeast cytochrome bc_1 complex is an early event and is independent of Rip1. *Biochim. Biophys. Acta* **1853,** 987–995
27. Zara, V., Conte, L., and Trumpower, B. L. (2007) Identification and characterization of cytochrome bc_1 subcomplexes in mitochondria from yeast with single and double deletions of genes encoding cytochrome bc_1 subunits. *FEBS J.* **274,** 4526–4539
28. Lombardi, A., Silvestri, E., Moreno, M., De Lange, P., Farina, P., Goglia, F., and Lanni, A. (2002) Skeletal muscle mitochondrial free-fatty-acid content and membrane potential sensitivity in different thyroid states: involvement of uncoupling protein-3 and adenine nucleotide translocase. *FEBS Lett.* **532,** 12–16
29. Zara, V., Conte, L., and Trumpower, B. L. (2009) Biogenesis of the yeast cytochrome bc_1 complex. *Biochim. Biophys. Acta* **1793,** 89–96
30. Monschau, N., Stahmann, K. P., Sahm, H., McNeil, J. B., and Bognar, A. L. (1997) Identification of *Saccharomyces cerevisiae* GLY1 as a threonine aldolase: a key enzyme in glycine biosynthesis. *FEMS Microbiol. Lett.* **150,** 55–60
31. Schlösser, T., Gätgens, C., Weber, U., and Stahmann, K. P. (2004) Alanine: glyoxylate aminotransferase of *Saccharomyces cerevisiae*-encoding gene AGX1 and metabolic significance. *Yeast* **21,** 63–73
32. Lee, J. C., Tsoi, A., Kornfeld, G. D., and Dawes, I. W. (2013) Cellular responses to L-serine in *Saccharomyces cerevisiae*: roles of general amino acid control, compartmentalization, and aspartate synthesis. *FEMS Yeast Res.* **13,** 618–634
33. Kastanos, E. K., Woldman, Y. Y., and Appling, D. R. (1997) Role of mitochondrial and cytoplasmic serine hydroxymethyltransferase isozymes in de novo purine synthesis in *Saccharomyces cerevisiae*. *Biochemistry* **36,** 14956–14964
34. Pasternack, L. B., Laude, D. A., Jr., and Appling, D. R. (1992) 13C NMR detection of folate-mediated serine and glycine synthesis in vivo in *Saccharomyces cerevisiae*. *Biochemistry* **31,** 8713–8719
35. Subramanian, M., Qiao, W. B., Khanam, N., Wilkins, O., Der, S. D., Lalich, J. D., and Bognar, A. L. (2005) Transcriptional regulation of the one-carbon metabolism regulon in *Saccharomyces cerevisiae* by Bas1p. *Mol. Microbiol.* **57,** 53–69
36. Benavides, J., Garcia, M. L., Lopez-Lahoya, J., Ugarte, M., and Valdivieso, F. (1980) Glycine transport in rat brain and liver mitochondria. *Biochim. Biophys. Acta* **598,** 588–594
37. Palmieri, F., and Monné, M. (2016) Discoveries, metabolic roles and diseases of mitochondrial carriers: A review. *Biochim. Biophys. Acta* **1863,** 2362–2378
38. Castegna, A., Scarcia, P., Agrimi, G., Palmieri, L., Rottensteiner, H., Spera, I., Germinario, L., and Palmieri, F. (2010) Identification and functional characterization of a novel mitochondrial carrier in *S. cerevisiae*. *J. Biol. Chem.* **285,** 17359–17370
39. Trotter, P. J., Adamson, A. L., Ghrist, A. C., Rowe, L., Scott, L. R., Sherman, M. P., Stites, N. C., Sun, Y., Tawiah-Boateng, M. A., Tibbetts, A. S., Wadington, M. C., and West, A. C. (2005) Mitochondrial transporters involved in oleic acid utilization and glutamate metabolism in yeast. *Arch. Biochem. Biophys.* **442,** 21–32
40. Dallabona, C., Marsano, R. M., Arzuffi, P., Ghezzi, D., Mancini, P., Zeviani, M., Ferrero, I., and Donnini, C. (2010) Sym1, the yeast ortholog of the MPV17 human disease protein, is a stress-induced bioenergetic and morphogenetic mitochondrial modulator. *Hum. Mol. Genet.* **19,** 1098–1107
41. Smith, P. M., Fox, J. L., and Winge, D. R. (2012) Biogenesis of the cytochrome bc_1 complex and role of assembly factors. *Biochim. Biophys. Acta.* **1817,** 276–286
42. Brachmann, C. B., Davies, A., Cost, G. J., Caputo, E., Li, J., Hieter, P., and Boeke, J. D. (1998) Designer deletion strains derived from *Saccharomyces cerevisiae* S288C: a useful set of strains and plasmids for PCR-mediated gene disruption and other applications. *Yeast.* **14,** 115–132
43. Sherman, F. (1991) Getting started with yeast. *Methods Enzymol.* **194,** 3–21
44. Damiano, F., Alemanno, S., Gnoni, G. V., and Siculella, L. (2010) Translational control of the sterol-regulatory transcription factor SREBP-1 mRNA in response to serum starvation or ER stress is mediated by an internal ribosome entry site. *Biochem. J.* **429,** 603–612
45. Rigiracciolo, D. C., Scarpelli, A., Lappano, R., Pisano, A., Santolla, M. F., De Marco, P., Cirillo, F., Cappello, A. R., Dolce, V., Belfiore, A., Maggiolini, M., and De Francesco, E. M. (2015) Copper activates HIF-1α/GPER/VEGF signalling in cancer cells. *Oncotarget* **6,** 34158–34177
46. Carrisi, C., Madeo, M., Morciano, P., Dolce, V., Cenci, G., Cappello, A. R., Mazzeo, G., Iacopetta, D., and Capobianco, L. (2008) Identification of the *Drosophila melanogaster* mitochondrial citrate carrier: bacterial expression, reconstitution, functional characterization, and developmental distribution. *J. Biochem.* **144,** 389–392
47. Iacopetta, D., Carrisi, C., De Filippis, G., Calcagnile, V. M., Cappello, A. R., Chimento, A., Curcio, R., Santoro, A., Vozza, A., Dolce, V., Palmieri, F., and Capobianco, L. (2010) The biochemical properties of the mitochondrial thiamine pyrophosphate carrier from *Drosophila melanogaster*. *FEBS J.* **277,** 1172–1181
48. Ersoy Tunalı, N., Marobbio, C. M., Tiryakioğlu, N. O., Punzi, G., Saygılı, S. K., Onal, H., and Palmieri, F. (2014) A novel mutation in the SLC25A15 gene in a Turkish patient with HHH syndrome: functional analysis of the mutant protein. *Mol. Genet. Metab.* **112,** 25–29
49. Madeo, M., Carrisi, C., Iacopetta, D., Capobianco, L., Cappello, A. R., Bucci, C., Palmieri, F., Mazzeo, G., Montalto, A., and Dolce, V. (2009) Abundant expression and purification of biologically active mitochondrial citrate carrier in baculovirus-infected insect cells. *J. Bioenerg. Biomembr.* **41,** 289–297
50. Lunetti, P., Cappello, A. R., Marsano, R. M., Pierri, C. L., Carrisi, C., Martello, E., Caggese, C., Dolce, V., and Capobianco, L. (2013) Mitochondrial glutamate carriers from *Drosophila melanogaster*: biochemical, evolutionary and modeling studies. *Biochim. Biophys. Acta* **1827,** 1245–1255
51. Daum, G., Böhni, P. C., and Schatz, G. (1982) Import of proteins into mitochondria: cytochrome b_2 and cytochrome *c* peroxidase are located in the intermembrane space of yeast mitochondria. *J. Biol. Chem.* **257,** 13028–13033
52. Ferramosca, A., and Zara, V. (2013) Biogenesis of mitochondrial carrier proteins: molecular mechanisms of import into mitochondria. *Biochim. Biophys. Acta* **1833,** 494–502
53. Pringle, J. R., Adams, A. E., Drubin, D. G., and Haarer, B. K. (1991) Immunofluorescence methods for yeast. *Methods Enzymol.* **194,** 565–602
54. Iacopetta, D., Lappano, R., Cappello, A. R., Madeo, M., De Francesco, E. M., Santoro, A., Curcio, R., Capobianco, L., Pezzi, V., Maggiolini, M., and Dolce, V. (2010) SLC37A1 gene expression is up-regulated by epidermal growth factor in breast cancer cells. *Breast Cancer Res. Treat.* **122,** 755–764
55. De Caroli, M., Lenucci, M. S., Manualdi, F., Dalessandro, G., De Lorenzo, G., and Piro, G. (2015) Molecular dissection of *Phaseolus vulgaris* polygalacturonase-inhibiting protein 2 reveals the presence of hold/release domains affecting protein trafficking toward the cell wall. *Front. Plant Sci.* **6,** 660
56. Villas-Bôas, S. G., Højer-Pedersen, J., Akesson, M., Smedsgaard, J., and Nielsen, J. (2005) Global metabolite analysis of yeast: evaluation of sample preparation methods. *Yeast* **22,** 1155–1169
57. De Benedetto, G. E., and Fanigliulo, M. (2009) A new CE-ESI-MS method for the detection of stable hemoglobin acetaldehyde adducts, potential biomarkers of alcohol abuse. *Electrophoresis.* **30,** 1798–1807
58. Materazzi, S., Napoli, A., Risoluti, R., Finamore, J., and D'Arienzo, S. (2014) Characterization of thermally induced mechanisms by mass spectrometry-evolved gas analysis (EGA-MS): a study of divalent cobalt and zinc biomimetic complexes with *N*-heterocyclic dicarboxylic ligands. *Int. J. Mass Spectrom.* **365,** 372–376
59. De Benedetto, G. E., Fico, D., Margapoti, E., Pennetta, A., Cassiano, A., and Minerva, B. (2013) The study of the mural painting in the 12th century monastery of Santa Maria delle Cerrate (Puglia-Italy): characterization of materials and techniques used. *J. Raman Spectrosc.* **44,** 899–904
60. Kranen, R. W., van Kuppevelt, T. H., Goedhart, H. A., Veerkamp, C. H., Lambooy, E., and Veerkamp, J. H. (1999) Hemoglobin and myoglobin content in muscles of broiler chickens. *Poult. Sci.* **78,** 467–476

61. Sinclair, P. R., Gorman, N., and Jacobs, J. M. (2001) Measurement of heme concentration. *Curr. Protoc. Toxicol.* Chapter 8: Unit 8.3
62. Benard, G., Faustin, B., Passerieux, E., Galinier, A., Rocher, C., Bellance, N., Delage, J. P., Casteilla, L., Letellier, T., and Rossignol, R. (2006) Physiological diversity of mitochondrial oxidative phosphorylation. *Am. J. Physiol. Cell Physiol.* **291,** C1172–C1182
63. Stendardi, A., Focarelli, R., Piomboni, P., Palumberi, D., Serafini, F., Ferramosca, A., and Zara, V. (2011) Evaluation of mitochondrial respiratory efficiency during in vitro capacitation of human spermatozoa. *Int. J. Androl.* **34,** 247–255
64. Cappello, A. R., Guido, C., Santoro, A., Santoro, M., Capobianco, L., Montanaro, D., Madeo, M., Andò, S., Dolce, V., and Aquila, S. (2012) The mitochondrial citrate carrier (CIC) is present and regulates insulin secretion by human male gamete. *Endocrinology* **153,** 1743–1754